# Passive intermodulation near-field measurements on microstrip lines

Sami Hienonen, Antti V. Räisänen

Radio Laboratory / SMARAD, Helsinki University of Technology, P.O.Box 3000, FIN-02015 HUT, Finland
Tel: +358 9 4512936, Fax: +358 9 4512152 E-mail address: Sami.Hienonen@hut.fi

***Abstract*— A passive intermodulation (PIM) near-field measurement equipment has been earlier designed in order to localise PIM sources in antennas and open transmission lines. The sensitivity of the scanner is −110 dBm with $P_{\mathrm{Tx}} = 2 \times 43$ dBm and it works in the GSM 900 frequency band. The antenna structure is scanned with a near-field probe and the results will reveal whether there are any PIM sources within the scanning area. However, the interpretation of the results is not always obvious. This paper introduces circuit model based equations which explain how the PIM electric and magnetic fields behave along a microstrip line. The differences in the reverse and forward traveling PIM waves caused by the asymmetry of the loading impedances are considered. Theory is compared with measurements including one and two PIM sources.**

## I. Introduction

Passive intermodulation (PIM) distortion continues to be a problem in wireless communication systems that utilize high power transmitters and sensitive receivers [1], [2]. The GSM system is especially problematic, since the base stations use several simultaneous narrow band carriers and their third-order intermodulation signals fall into the frequency band of the receiver. Base station antennas are typically subject to the PIM specification of −110 dBm with $2 \times 43$ dBm transmit power, which is not trivial to fulfil. The sources of PIM distortion are typically slightly nonlinear metal-metal junctions or magnetic materials [3]. In a base station antenna, these sources can be located in the antenna connector, antenna elements or in the feeding network, which is typically implemented as a coaxial cable or as a microstrip line. Depending on the manufacturing techniques, there are various junctions in the feed line that are potential PIM sources. The localisation of a PIM source by experiments is time consuming and often very difficult.

The reverse and forward PIM level of a device can be measured with a dedicated PIM analyser, but it does not reveal where the PIM distortion is generated. The PIM near-field measurement equipment described in [4] can be used to localise PIM sources in antennas and open transmission lines, see the block diagram in Fig. 1. The antenna structure is scanned with a near-field probe and the results will show whether there are any PIM sources in the scanning area. The interpretation of the results is not always obvious and, therefore, this paper explains how the PIM electric and magnetic fields behave along a microstrip line in case of one and two sources.

The source and load impedances seen by the PIM source cause the reverse and forward traveling voltage waves to differ. This can be seen both in the near-field measurements as well as on the reverse and forward PIM level measurements. An equation for the PIM voltage along a transmission line is given and the differences between the reverse and forward traveling waves are considered. Also, the case of two PIM sources is discussed.

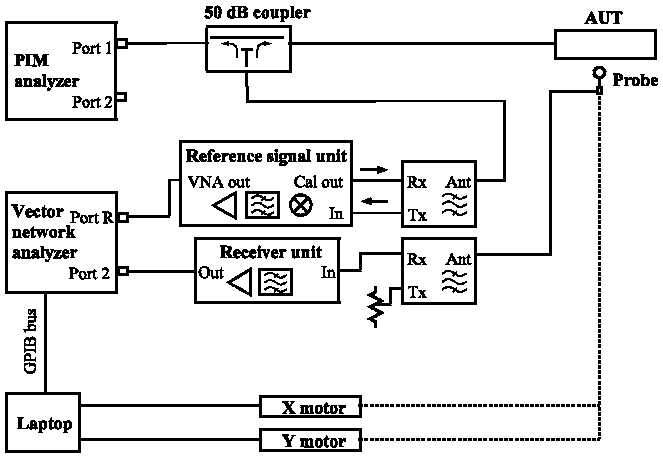


Fig. 1. Block diagram of the PIM near-field scanner.

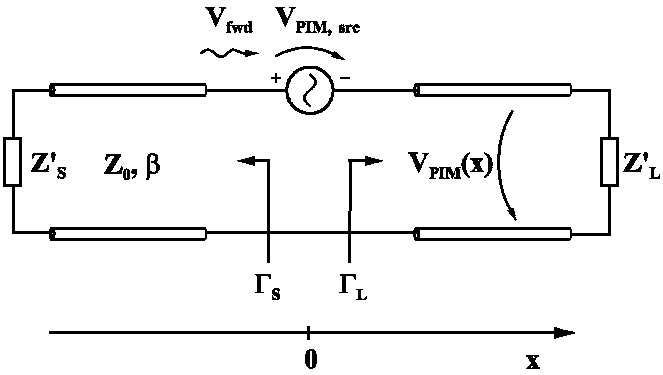


Fig. 2. Equivalent circuit of the PIM source in a microstrip line.

## II. Circuit model of PIM source

A simple circuit model of a PIM source described and verified in [5] is used to interpret the PIM near-field measurement results on microstrip lines. The model takes into account the source and load impedances seen by the PIM source, see Fig. 2. In the model, the incident voltage wave $V_{\mathrm{fwd}}$ induces the current $I$ to flow through the PIM source, which is assumed to obey the third-order Taylor polynomial model. The simplifying assumptions are that the impedance of the PIM source is negligible compared with the system impedance and that the PIM source is in series with the lossless transmission line.

The PIM voltage along the transmission line with a PIM

source at $x_0 = 0$ is

$$V_{\mathrm{PIM}}(x) = \begin{cases} V^- e^{j\beta x}(1+\Gamma_{\mathrm{s}} e^{-j2\beta x}), & x < 0, \\ V^+ e^{-j\beta x}(1+\Gamma_{\mathrm{L}} e^{j2\beta x}), & x > 0, \end{cases} \quad (1)$$

where $\beta$ is the propagation constant of the transmission line, $\Gamma_{\mathrm{s}}$ and $\Gamma_{\mathrm{L}}$ are the source and load reflection coefficients seen by the PIM source at the intermodulation frequency $f_3 = 2f_1 - f_2$. The reverse and forward traveling PIM voltage waves are

$$V^- = \frac{V_{\mathrm{PIM,src}}}{2} \frac{1-\Gamma_{\mathrm{L}}}{1-\Gamma_{\mathrm{s}}\Gamma_{\mathrm{L}}}, \quad (2)$$

$$V^+ = -\frac{V_{\mathrm{PIM,src}}}{2} \frac{1-\Gamma_{\mathrm{s}}}{1-\Gamma_{\mathrm{s}}\Gamma_{\mathrm{L}}}. \quad (3)$$

The voltage $V_{\mathrm{PIM,src}}$ across the PIM source and the current at the transmitting frequencies are

$$V_{\mathrm{PIM,src}} = \frac{3a_3}{4} I^2(f_1) I^*(f_2), \quad (4)$$

$$I(f) = \frac{V_{\mathrm{fwd}}(f)}{Z_0} \frac{1-\Gamma_{\mathrm{L}}(f)}{1-\Gamma_{\mathrm{s}}(f)\Gamma_{\mathrm{L}}(f)}, \quad (5)$$

where $a_3$ is the coefficient from the Taylor polynomial model of the PIM source and $Z_0$ is the impedance of the transmission line. The asterisk denotes the complex conjugate. Similar equations can be written for the PIM current, except that there is no sign change at $x = 0$.

### A. Reverse and forward PIM

It can be seen from (1) that the voltage waves on each side of the PIM source are approximately out-of-phase and that the exact phase difference depends on the source and load impedances. Their amplitudes will also be different. The ratio of the reverse and forward traveling PIM voltages at the PIM source is simply

$$\frac{V^-}{V^+} = -\frac{1-\Gamma_{\mathrm{L}}}{1-\Gamma_{\mathrm{s}}}. \quad (6)$$

The maximum possible differences in the amplitude and phase are plotted in Fig. 3 versus return loss when $|\Gamma_{\mathrm{s}}| = |\Gamma_{\mathrm{L}}|$. It should be noted that the amplitude and phase maxima are not achieved at the same time. The difference in the reverse and forward voltage can be up to $\pm 3$ dB when the return losses of the source and load are 15 dB. Although the plot shows the worst case, it is a reasonable approximation of the maximum difference over the whole frequency band of the device.

Essentially the same effect will be seen in the reverse and forward PIM power measurement. The PIM power dissipated in the source and load impedances are

$$P_{\mathrm{rev}} = \frac{|V^-|^2}{2Z_0}(1-|\Gamma_{\mathrm{s}}|^2), \quad (7)$$

$$P_{\mathrm{fwd}} = \frac{|V^+|^2}{2Z_0}(1-|\Gamma_{\mathrm{L}}|^2). \quad (8)$$

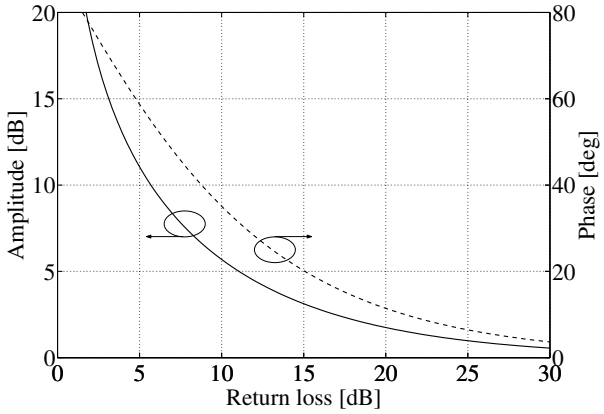


Fig. 3. Maximum possible difference of the reverse and forward traveling PIM voltages calculated from (6) with $|\Gamma_{\mathrm{s}}| = |\Gamma_{\mathrm{L}}|$.

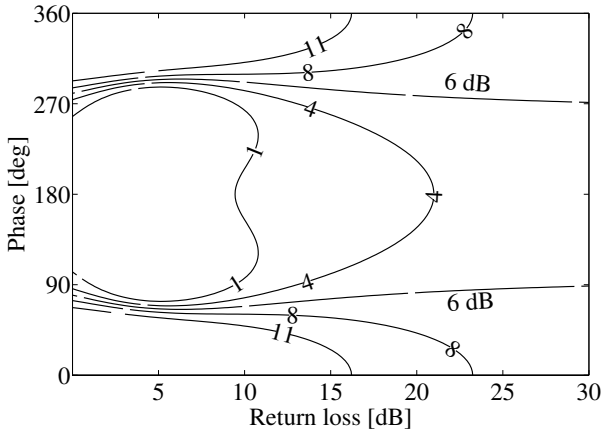


Fig. 4. Ratio of the forward traveling PIM voltage caused by two and one PIM sources versus the load reflection coefficient. Calculated from (9) with $a = \lambda/4$. The ratio is plotted in decibels.

### B. Two PIM sources

The sum of the voltage waves generated by two similar PIM sources in a transmission line can be calculated from (2)–(5) by weighting the reflection coefficients and $V_{\mathrm{fwd}}$ with proper phase factors. The resulting equations are lengthy, but the behaviour of the sum can be studied with approximations. For example, the ratio of the forward traveling PIM voltage wave caused by two and one PIM sources is

$$\frac{V_1^+ e^{-j\beta a} + V_2^+}{V_1^+ e^{-j\beta a}} = 1 + \frac{(1-\Gamma e^{j2\beta a})^2(1-\Gamma e^{-j2\beta a})}{(1-\Gamma)^3}, \quad (9)$$

when $\Gamma_{\mathrm{s}} = 0$, $\Gamma = \Gamma_{\mathrm{L}}(f_1) = \Gamma_{\mathrm{L}}^*(f_2)$, $\beta = \beta(f_1) = \beta(f_2) = \beta(f_3)$. The separation between the PIM sources is $a$.

This ratio is plotted versus the load reflection coefficient in Fig. 4, when $a = \lambda/4$. In this simplified case, the forward PIM level of two identical PIM sources is 2.5 to 12 dB higher than that of one PIM source, when the return loss is 15 dB. The difference will not be so high when the exact equation is used with practical reflection coefficients. However, the difference will deviate from the usual assumption of 6 dB, which is the case when the load and source are perfectly matched. It is also to be noted, that the forward PIM level depends on the electrical distance between the PIM sources when the loading impedances are taken into account.

### C. Normalisation

In order to compare the PIM near-field data with the reverse PIM measurement, a calibration measurement is needed [4]. In calibration, a known signal is fed to the device under test (DUT). The calibration signal voltage along the transmission line is

$$V_{\mathrm{cal}}(x) = V_{\mathrm{cal}}^{+} e^{-j\beta x} \frac{1+\Gamma_{\mathrm{L}} e^{j2\beta x}}{1-\Gamma_{\mathrm{s}}\Gamma_{\mathrm{L}}}, \tag{10}$$

where $V_{\mathrm{cal}}^{+}$ is the incident calibration voltage wave at the PIM source and the other parameters are shown in Fig. 2. Then, the normalised PIM voltage is

$$V_{\mathrm{IM3,DUT}}(x) = \frac{V_{\mathrm{PIM}}(x)}{V_{\mathrm{cal}}(x)} \left|V_{\mathrm{cal}}^{+}\right| =$$

$$\begin{cases} \dfrac{V_{\mathrm{PIM,src}}}{2} e^{j2\beta x}(1-\Gamma_{\mathrm{L}}) \dfrac{1+\Gamma_{\mathrm{s}} e^{-j2\beta x}}{1+\Gamma_{\mathrm{L}} e^{j2\beta x}} e^{j\phi}, & x<0, \\ -\dfrac{V_{\mathrm{PIM,src}}}{2}(1-\Gamma_{\mathrm{s}}) e^{j\phi}, & x>0, \end{cases} \tag{11}$$

where $\phi$ is an unknown constant.

Thus, it can be seen that the normalised PIM voltage with $x<0$ and $x>0$ are comparable with the reverse and forward PIM power in (7)–(8), respectively. Furthermore, $V_{\mathrm{IM3,DUT}}$ is constant between the PIM source and the load, whereas it will fluctuate between the signal and PIM source.

## III. Measurements

Different kinds of PIM sources on a microstrip line have been scanned with both electric and magnetic field probes. Pieces of various materials were inserted below the strip or within the strip in order to cause PIM distortion. It was found out that most of the PIM sources were in series with the microstrip line. Only a diode in the vicinity of the strip was found to be in parallel. The transmitting power was $2\times 43$ dBm and the frequencies were $f_1 = 935$ MHz and $f_2 = 960$ MHz in the measurements.

An example of the scan along the microstrip line with a PIM source is shown in Fig. 5. It can be seen that the $E_z$-field has a discontinuity at the source as given in (1). The $H_y$-field is continuous over the source and there is a peak in the near-field of the source, which naturally cannot be predicted by the circuit model. In both the electric and magnetic field the slope of the phase points towards the PIM source as expected. The estimated phase differences between the forward and reverse PIM waves are 172 and 18 degrees for $E_z$ and $H_y$-fields, respectively.

An extreme case of two PIM sources having equal amplitudes is shown in Fig. 6. Here, one PIM source is located in the feeding cable before the microstrip whereas the other is located at $x = 358$ mm in the microstrip line. Amplitude minima and maxima cannot be used anymore in determining the location of the PIM source. However, the slope of the PIM phase unmasks the latter PIM source. It is also seen that the amplitude between $x = 360$ and 450 mm is 3 to 5 dB lower than the maxima in the standing wave pattern. This can be understood by the effect of the loading impedances as explained in Sect. II-B.

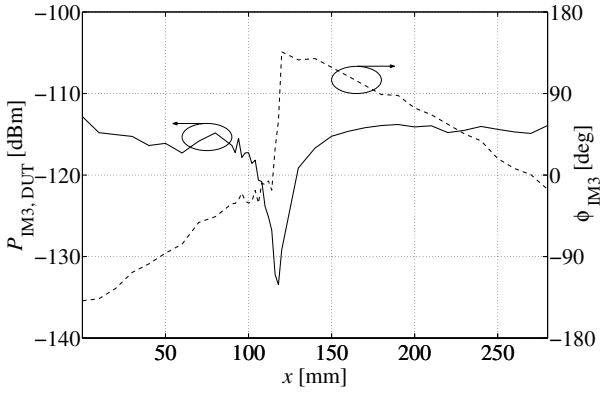


(a) $E_z$-field

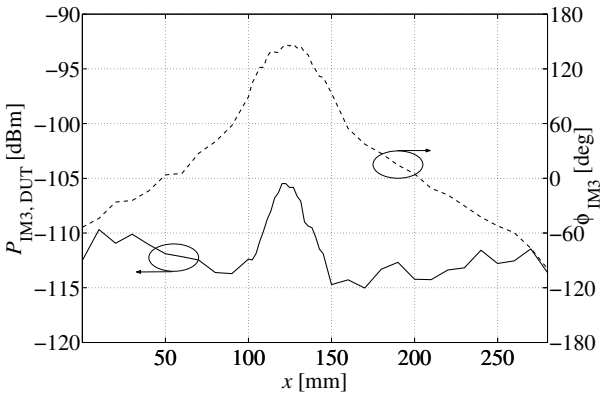


(b) $H_y$-field

Fig. 5. One PIM source. Normalised PIM level $P_{\mathrm{IM3,DUT}}$ and PIM phase $\phi_{\mathrm{IM3}}$ along a microstrip line. A piece of stainless steel below the strip at $x =$ 118 mm. Reverse PIM level $-111$ dBm, $P_{\mathrm{Tx}} = 2\times 43$ dBm, $f_{\mathrm{IM3}} = 910$ MHz.

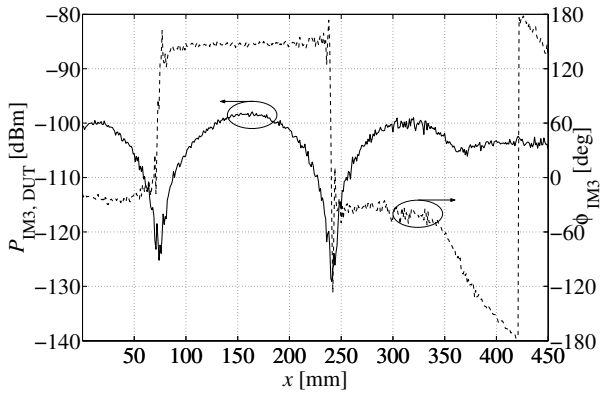


Fig. 6. Two PIM sources. Normalised PIM level $P_{\mathrm{IM3,DUT}}$ and PIM phase $\phi_{\mathrm{IM3}}$ along a microstrip line. An N-N adapter is located left from the microstrip and a piece of ferrite is located at $x = 358$ mm. $H_y$-field.

## IV. Conclusion

Passive intermodulation near-field scanner can be used to localise PIM sources in antennas and open transmission lines, but the interpretation of the measurement results is not always obvious. Equations for the PIM voltage along a transmission line has been given and the effect of the loading impedances seen by the PIM source is considered. The reverse and forward traveling waves will, in general, differ both in amplitude and in phase. The theoretical PIM signal characteristics were compared with the near-field measurement results of PIM sources in a microstrip line. It was also found out that the ratio of the forward traveling PIM voltage wave caused by two and

one PIM sources deviates from the usual assumption of 6 dB. The ratio also depends on the electrical length between the sources.

The loading impedance effects can be several decibels when the return loss of the source or load is less than 20 dB, a condition that is often met in base station antennas and filters. Therefore, the loading impedances should be taken into account when performing passive intermodulation measurements or developing low-PIM devices.

## ACKNOWLEDGEMENT

This work was supported in part by the Nokia Foundation, the Jenny and Antti Wihuri Foundation, the Emil Aaltonen Foundation, and by the Academy of Finland and Tekes through their Center of Excellence program.

## REFERENCES

[1] P. L. Lui, "Passive intermodulation interference in communication systems," *Electronics and Communication Engineering Journal*, vol. 2, pp. 109–118, June 1990.

[2] R. Singh and E. Hunsaker, "Systems methodology for PIM mitigation of communications satellites," in *Proceedings of the 4th International Workshop on Multipactor, Corona and Passive Intermodulation in Space RF Hardware (MULCOPIM2003)*, ESTEC, Noordwijk, Netherlands, Sept. 8–11, 2003, CD-ROM.

[3] B. G. M. Helme, "Interference in telecomm systems, from passive intermodulation product generation: an overview," in *Proceedings of the 22nd Antenna Measurement Techniques Association Annual Symposium (AMTA 2000)*, Philadelphia, Oct. 16–20, 2000, pp. 143–149.

[4] S. Hienonen, V. Golikov, P. Vainikainen, and A. V. Räisänen, "Near-field scanner for the detection of passive intermodulation sources in base station antennas," *IEEE Trans. Electromagn. Compat.*, to be published.

[5] S. Hienonen and A. V. Räisänen, "Effect of load impedance on passive intermodulation measurements," *Electronics Letters*, vol. 40, no. 4, pp. 245–247, Feb. 2004.